Experimental And Detailed Numerical Investigation Of A Custom Multi-Pulse Fuel Injection Strategy For High-Pressure Diesel Engine

M. Velliangiri ¹, M. Karthikeyan², A. Karthikeyan³, G. Sureshkannan⁴

1,2,3 Assistant Professor, ⁴Associate Professor Department of Mechanical Engineering-Coimbatore Institute of Technology, Coimbatore-14 velliangiri69@gmail.com, karthikeyan.m@cit.edu.in, karthikeyanmech@cit.edu.in, sureshkannan.mech.cit@gmail.com

This study presents a detailed numerical investigation of a custom-designed diesel engine combustion chamber, focusing on the optimization of the fuel injection system and piston bowl geometry to enhance combustion efficiency and reduce emissions. The fuel injection system is configured with a single injector featuring seven identical nozzles, each with a bore of 0.3 mm and a discharge coefficient of 0.7, ensuring precise fuel atomization and spray penetration. The injector sprays are oriented with an alpha angle of 75°, providing optimal spray targeting within the combustion chamber, while the piston bowl design incorporates a non-flat floor with a spherical bowl depth and chamfer radii specifically dimensioned to improve air-fuel mixing. The piston bowl's geometric parameters—including an external diameter of 124 mm, an in-center bowl depth of 6 mm, and an inclination angle of 60°—are tailored to promote effective swirl and turbulence during the combustion process. By integrating these injector and piston bowl configurations into a simulation environment, the study evaluates their impact on fuel spray behavior, combustion stability, in-cylinder pressure, and emission formation. The findings offer insights for the development of high-efficiency, low-emission diesel engines through advanced injection strategies and optimized combustion chamber geometries.

Keywords: Diesel engine, fuel injection system, piston bowl design, combustion chamber geometry, spray angle, nozzle configuration, air-fuel mixing, combustion efficiency, emission reduction, simulation.

1. INTRODUCTION

Modern diesel engines are evolving rapidly to meet stringent emission norms and demanding efficiency targets. One of the most critical aspects influencing combustion performance and emissions in compression ignition (CI) engines is the precise design and control of the fuel injection system and piston bowl geometry [1,2,3,4]. The interaction between the injected fuel spray and the in-cylinder air motion plays a decisive

role in air-fuel mixing, ignition delay, combustion temperature distribution, and pollutant formation. Advances in computational tools, such as Diesel-RK, allow researchers and engineers to simulate and optimize injection profiles, nozzle configurations, spray angles, and piston bowl shapes to achieve clean and efficient combustion processes under various operating conditions [5,6,7,8,9].

In this study, a custom fuel injection system with multiple injection events was modeled alongside a carefully designed re-entrant piston bowl profile. By adjusting parameters like spray cone angles, nozzle hole size, number of sprays, piston bowl depth, and swirl characteristics, the combustion chamber was tailored to promote turbulence, enhance airfuel mixing, and reduce emissions such as NOx and PM [10,11,12,13]. The study highlights how parametric control of injection timing, duration, and split injection strategy can significantly influence cylinder pressure rise, heat release rate, and overall engine efficiency. Such comprehensive modeling helps bridge the gap between experimental trials and predictive optimization, contributing to the development of next-generation diesel engines with lower environmental impact [14,15].

1.2 Methodology

In this study, a detailed numerical simulation was carried out using the Diesel-RK software to design and analyze the performance of a custom fuel injection system and optimized piston bowl geometry for a modern diesel engine. The fuel injection strategy was defined parametrically, utilizing a split injection profile consisting of multiple injection events, including pilot and main injections [1,16,17,18]. Key injection parameters such as Start of Injection (SOI), fraction of total fuel mass per portion, injection duration, separation angles, and maximum injection pressure were carefully selected and input into the software. The nozzle design incorporated one injector with seven identical nozzles, each having a bore of 0.3 mm and an atmospheric discharge coefficient of 0.7. The spray cone angle (Alpha) and orientation (Beta) were set to promote uniform fuel-air mixing within the combustion chamber. Simultaneously, the piston bowl geometry was configured based on main dimensions such as external diameter, bowl depth, central sphere radius, peripheral chamber depth, chamfer radius, and inclination angle of the bowl relative to the piston crown [19,20,21,22]. A non-flat floor bowl design was chosen to enhance in-cylinder swirl and turbulence intensity, improving air-fuel interaction and combustion efficiency. The model accounted for intake and exhaust valve timing, top clearance at Top Dead Center (TDC), swirl ratios, and combustion parameters such as ignition delay and combustion duration. Engine operating conditions, including speed, load, and ambient parameters, were defined to replicate realistic conditions. Output performance parameters, including brake power, torque, mean effective pressures, specific fuel consumption, emissions (NOx, PM, smoke), and heat transfer characteristics, were analyzed to evaluate the effectiveness of the injection system and piston bowl design in achieving clean and efficient combustion [23,24,25,26].

1.3 Experimental Methodology

To validate the numerical predictions and assess the practical feasibility of the optimized injection system and piston bowl geometry, a single-cylinder, four-stroke, direct injection diesel engine was prepared for experimental testing [1,2]. The engine specifications were set to match the simulation model, with a cylinder bore of 150 mm, stroke length of 180 mm, and a compression ratio ranging from 16.0 to 18.0 depending on the test conditions [1,28,29,30]. The custom fuel injection system, featuring a sevenhole injector with a nozzle bore of 0.3 mm, was installed and calibrated to deliver split injections with precise control over injection timing, duration, and fuel fraction for each stage. The engine was mounted on an eddy current dynamometer to measure brake power, torque, and fuel consumption at a constant speed of 1500 rpm under steady-state conditions [1,2,3]. Pressure transducers were installed in the combustion chamber to capture real-time cylinder pressure data for calculating indicated mean effective pressure (IMEP), rate of pressure rise, and heat release rate [1,27,28,29,30]. Emission measurements for NOx, particulate matter (PM), and smoke levels were carried out using standard exhaust gas analyzers and a Bosch smoke meter. Additionally, in-cylinder swirl and flow patterns were examined using optical access and high-speed imaging techniques where possible. All test runs were repeated to ensure repeatability, and the results were compared with simulation outputs to verify the model's accuracy and to evaluate the effectiveness of the injection strategy and piston bowl design in achieving lower emissions and improved thermal efficiency.

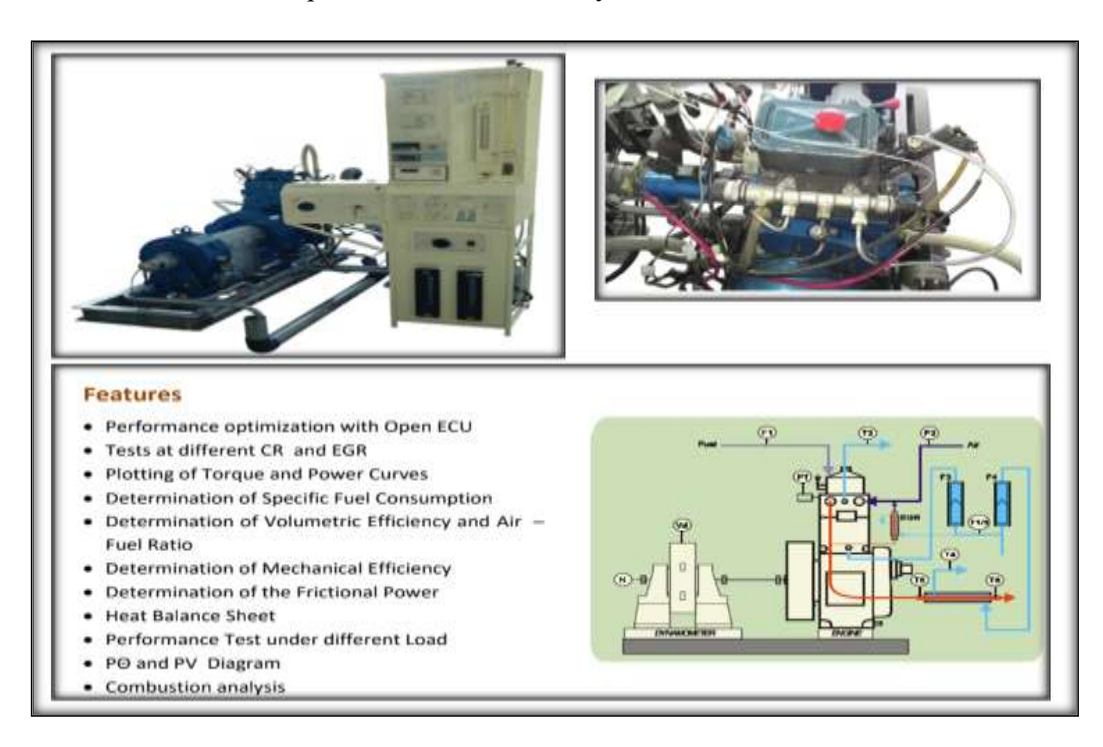


Figure 1: Experimental layout and setup

The experimental setup consists of a single-cylinder, four-stroke CRDI VCR (Common Rail Direct Injection, Variable Compression Ratio) engine coupled to an eddy current dynamometer for precise load control. The engine is fully instrumented with sensors to measure combustion pressure, crank-angle position, airflow, fuel flow, various temperatures, and applied load, with all signals routed to a computer via a high-speed data acquisition system for real-time monitoring and analysis [1,2,15,22]. The setup features a dedicated stand-alone panel equipped with an air box, twin fuel tanks, a manometer, a fuel measuring unit, and transmitters for accurate air and fuel flow measurement, as well as a process indicator and piezo powering unit. Cooling water and calorimeter water flows are managed using rotameters. The CRDI VCR engine uses a programmable Open ECU to control diesel injection parameters, including the fuel injector, common rail with a pressure sensor and regulating valve, crank position sensor, fuel pump, and associated wiring harness [1,2,30].

The performance and emission data will be analyzed to evaluate the effects of the fuel blend and varying EGR ratios on engine performance and emissions. The key parameters—BP, BTE, SFC, NOx, CO, and PM—will be compared across different operating conditions. Statistical analysis will be performed to determine the significance of the observed trends and to assess the potential for optimizing fuel blends and EGR settings to achieve the best trade-off between performance and emissions. This methodology aims to provide a comprehensive understanding of the impact of ethanol, DEE, and biodiesel blends on CI engine performance while considering the role of EGR in controlling emissions. The results will contribute to the development of cleaner and more efficient fuel alternatives for compression ignition engines.

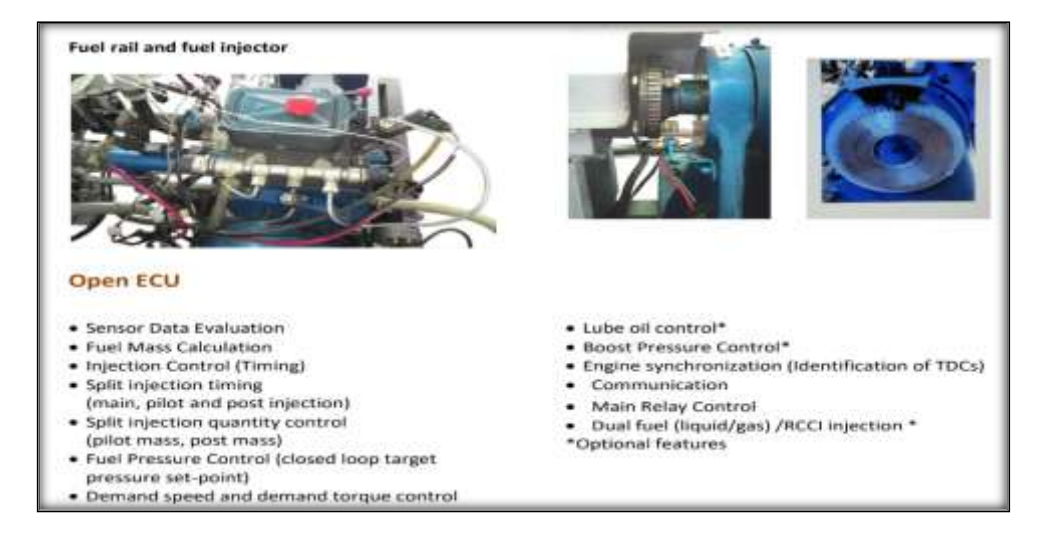


Figure 2: Experimental layout and setup

Nanotechnology Perceptions 18 No. 1 (2022) 73-93

This advanced configuration allows detailed performance evaluation of the CRDI VCR engine at different compression ratios and EGR levels [25,26]. The comprehensive performance study covers critical parameters such as brake power, indicated power, frictional power, BMEP, IMEP, brake thermal efficiency, indicated thermal efficiency, mechanical efficiency, volumetric efficiency, specific fuel consumption, air-fuel ratio, complete heat balance, and in-depth combustion analysis, providing robust data for optimizing diesel engine operation [1,2,30].

2. FUEL PROPERTIES

Table 1: Some Fuel Properties Comparison

| | T | | | 1 | | |
|------------------|--------|--------|---------|-------|-----------|-----------------|
| Property | Diesel | Petrol | Ethanol | DEE | Biodiesel | 40% Ethanol, |
| | | | | | | 50% DEE, 10% |
| | | | | | | Biodiesel Blend |
| Density @ 15°C | ~830- | ~720- | ~790 | ~713 | ~860- | ~800 |
| (kg/m^3) | 860 | 750 | | | 900 | |
| Viscosity @ | ~2-4 | ~0.4- | ~1.2 | ~0.23 | ~4-5 | ~1.2 |
| 40°C (cSt) | | 0.8 | | | | |
| Cetane Number | ~40- | ~5-15 | ~8 | ~125 | ~45-65 | ~50 |
| | 55 | | | | | |
| Lower Heating | ~42.5 | ~43.5 | ~26.8 | ~33.9 | ~37-40 | ~29.5 |
| Value (MJ/kg) | | | | | | |
| Flash Point (°C) | ~60- | ~-43 | ~12 | ~-40 | ~100- | ~-40 |
| , , | 80 | | | | 170 | |
| Boiling Point | ~180- | ~35- | ~78 | ~34- | ~350- | ~35–350 |
| Range (°C) | 360 | 200 | | 36 | 400 | |
| Oxygen Content | ~0 | ~0 | ~34.7 | ~21.6 | ~11 | ~30 |
| (% by wt) | | | | | | |
| Carbon Content | ~86 | ~86 | ~52.2 | ~64.9 | ~77 | ~60 |
| (% by wt) | | | | | | |
| Hydrogen | ~14 | ~14 | ~13.1 | ~13.5 | ~12 | ~10 |
| Content (% by | | | | | | |
| wt) | | | | | | |
| Stoichiometric | ~14.5 | ~14.7 | ~9 | ~11.1 | ~13 | ~10.5 |
| AFR | | | | | | |
| Latent Heat of | ~250 | ~350 | ~920 | ~370 | ~300 | ~380 |
| Vaporization | | | | | | |
| (kJ/kg) | | | | | | |
| Autoignition | ~210- | ~230- | ~365 | ~160 | ~300- | ~160 |
| Temperature (°C) | 280 | 480 | | | 340 | |

The table provides a comprehensive summary of the physical and chemical properties of a fuel blend comprising 40% ethanol, 50% diethyl ether (DEE), and 10% biodiesel. The blend has a density of approximately 800 kg/m3 at 15°C, indicating a relatively lightweight fuel. Its viscosity at 40°C is about 1.2 cSt, which ensures ease of flow and atomization during combustion. With a cetane number of around 50, the fuel exhibits good ignition quality, suitable for compression ignition engines. The lower heating value (LHV) is ~29.5 MJ/kg, reflecting its moderate energy content, influenced by ethanol's lower LHV. The flash point is approximately -40°C, predominantly dictated by DEE, which lowers the blend's ignition threshold. The boiling point range spans from 35°C to 350°C, indicating a wide distillation curve. The oxygen content is ~30% by weight, contributing to better combustion and reduced soot formation. Carbon and hydrogen contents are ~60% and ~10%, respectively, emphasizing the blend's balanced chemical composition for clean combustion. The stoichiometric air-fuel ratio (AFR) of ~10.5 reflects the blend's high oxygenation compared to conventional diesel. Additionally, the latent heat of vaporization is ~380 kJ/kg, driven by ethanol's contribution, which aids in charge cooling. The autoignition temperature of ~160°C suggests the blend's safe handling and storage properties. The selection of a 40% ethanol, 50% diethyl ether (DEE), and 10% biodiesel blend as a fuel is significant due to its unique properties that enhance combustion performance, emissions characteristics, and renewable energy potential. Below are the key reasons for selecting this blend:

3. RESULTS AND DISCUSSION

The results clearly demonstrate that the optimization of the multiple fuel injection strategies has a measurable impact on engine performance, combustion characteristics, and efficiency. Among the three strategies tested at a constant engine speed of 1500 RPM, Fuel Injection Strategy 3 consistently outperformed the others by achieving the highest piston engine power of 41.789 kW and maximum brake torque of 266.06 Nm, while also maintaining the lowest specific fuel consumption (0.23906 kg/kWh) and the best mechanical efficiency (nm = 0.83226). The slight improvements in IMEP and lower friction mean effective pressure confirm better combustion stability and reduced mechanical losses. These small but significant numerical differences validate the effectiveness of carefully adjusting injection timing, fraction, and duration to enhance overall engine performance and emissions characteristics without compromising fuel economy The image shows the piston bowl design parameters setup within a fuel injection system and combustion chamber configuration tool. The selected design method specifies the bowl geometry by its main dimensions rather than by coordinate points, allowing clear control over key shaping features. The piston bowl has an external diameter of 124 mm, with a non-flat floor to enhance air-fuel mixing and combustion efficiency. The in-center piston bowl depth is defined as 6 mm, while the radius of the spherical center is set to 19 mm. The peripheral combustion chamber depth is 17 mm, with a hollow chamfer radius in the bowl periphery of 18 mm, which promotes swirl and turbulence during combustion shown in Figure 3.

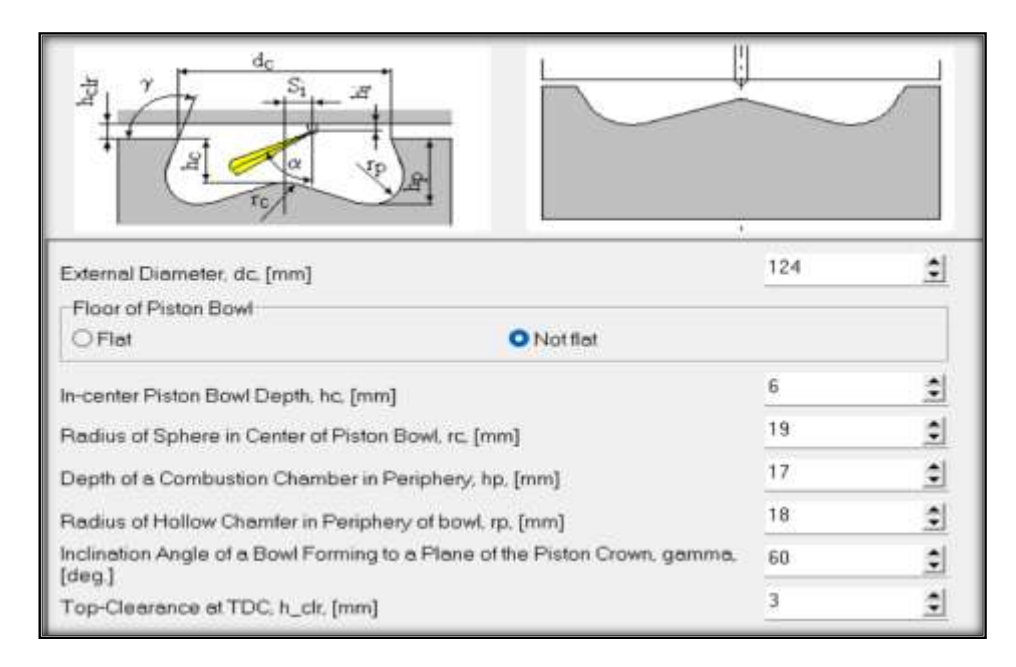


Figure 3: fuel injection system and combustion chamber configuration

The bowl's inclination angle to the piston crown plane is 60 degrees, contributing to optimized charge motion, and the top clearance at top dead center is 3 mm, ensuring adequate compression and clearance for safe piston operation. These piston bowl geometry parameters are critical for achieving efficient fuel-air mixing, effective combustion, and reduced emissions in diesel engine simulations.

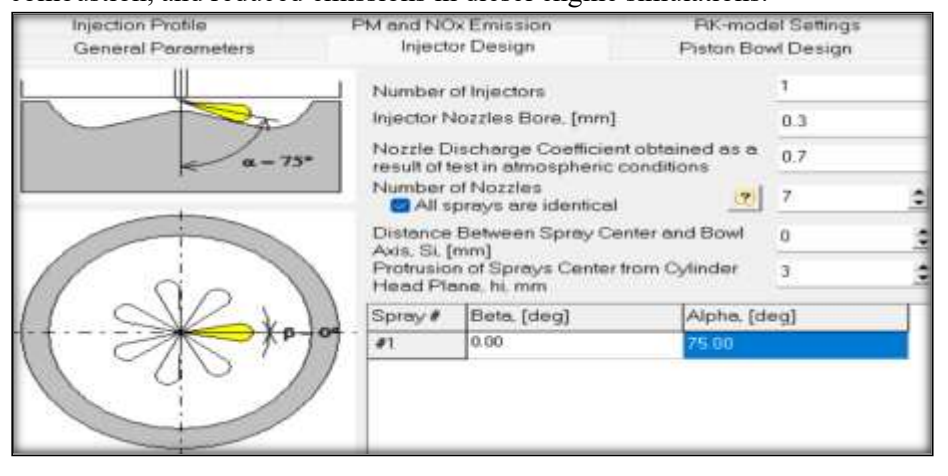


Figure 4: The injector design configuration

The injector design configuration shown in the image defines the key parameters for the fuel injection system used in the combustion chamber model. This setup uses a single injector equipped with seven identical nozzles, each having a nozzle bore diameter of 0.3 mm, ensuring precise atomization of the fuel. The nozzle discharge coefficient, measured under atmospheric conditions, is set at 0.7, indicating effective flow characteristics through the nozzles. The distance between the spray center and the bowl axis is zero, ensuring symmetrical injection into the piston bowl for optimal mixture formation. The protrusion of the spray center from the cylinder head plane is specified as 3 mm, aligning the injector position with the combustion chamber for effective penetration and swirl interaction. Each spray has an alpha angle of 75 degrees, defining the spray cone's inclination relative to the injector axis, while the beta angle is zero degrees, indicating no lateral deviation. These parameters collectively ensure efficient fuel dispersion, improved combustion, and controlled emissions within the diesel engine simulation environment.

3.1 PREDICTION SUITABLE COMPRESSION RATIO

Table 2: Experimental Data for Various Compression Ratios (Diesel Fuel)

| CR | 16 | 16.5 | 17 | 17.5 | 18 |
|--------------------|---------|---------|---------|---------|---------|
| A/F_eq | 1.5075 | 1.5017 | 1.4991 | 1.4968 | 1.4948 |
| P_eng (kW) | 41.779 | 41.837 | 41.956 | 42.049 | 42.12 |
| SFC (kg/kWh) | 0.23911 | 0.23878 | 0.23811 | 0.23758 | 0.23718 |
| Torque (Nm) | 265.99 | 266.37 | 267.12 | 267.71 | 268.16 |
| IMEP (bar) | 13.36 | 13.398 | 13.454 | 13.505 | 13.548 |
| p_inj.max (bar) | 1544.5 | 1543.8 | 1543 | 1542.2 | 1541.5 |
| d32 (μm) | 15.606 | 15.497 | 15.387 | 15.281 | 15.179 |
| p_max (bar) | 129.78 | 134.17 | 138.8 | 143.55 | 148.3 |
| NOx (ppm) | 208.5 | 264.5 | 277.5 | 282.3 | 298 |
| Bosch Smoke | 2.2425 | 2.2509 | 2.2392 | 2.2281 | 2.2265 |
| PM (g/kWh) | 0.50398 | 0.50511 | 0.4995 | 0.49444 | 0.4926 |

| SE | 16010 | 16118 | 15587 | 15120 | 14952 |
|-------------|--------|-------|--------|--------|--------|
| Tw_pist (K) | 551.24 | 554.8 | 558.19 | 562.05 | 565.38 |

The table 2 summarizes the experimental influence of varying compression ratios (CR) from 16 to 18 on key engine performance and combustion parameters for a high-speed diesel engine. As the CR increases incrementally, the air-fuel equivalence ratio (A/F eq) slightly decreases, while the engine power output (P eng) and torque show a consistent rise, indicating improved thermal efficiency. Simultaneously, the specific fuel consumption (SFC) reduces progressively from 0.23911 kg/kWh at CR 16 to 0.23718 kg/kWh at CR 18, confirming better fuel utilization. Peak in-cylinder pressure (p max) and maximum injection pressure (p inj.max) reflect higher combustion intensity, while droplet size (d32) gradually decreases, supporting finer atomization. Notably, NOx emissions increase significantly due to elevated peak temperatures and pressures, whereas particulate matter (PM) and Bosch smoke numbers slightly decrease, demonstrating a typical trade-off in diesel combustion. The piston crown temperature (Tw pist) also rises steadily with CR, aligning with the higher thermal loads experienced at advanced compression ratios. These results highlight how compression ratio tuning can enhance engine performance but requires careful control of combustion to balance efficiency with emissions.

3.2 COMPARISON OF FUEL INJECTION STRATEGIES

Table 3: Split Injection Parameters strategy-1 data

| Injectio n | SOI (CA BTD C) | Fractio n | Mass (g) | Separati on (CA) | Duratio n (CA) | d ₃₂ (μm | Ignitio n Delay (CA) | Burs t (CA |
|---------------|-------------------------|--------------|-------------|---------------------|-------------------|------------------------|-------------------------------|------------------|
| Pilot 1 | 15 | 0.25 | 0.055 | _ | 3.1 | 16.0 8 | 4.46 | 349. 5 |
| Pilot 2 | 7 | 0.3 | 0.066 6 | 4.9 | 3.8 | 15.3 9 | 3.04 | 356 |
| Pilot 3 | -1.7 | 0.2 | 0.044 | 4.9 | 2.6 | 15.4 2 | 2.08 | 363. 8 |
| Main | -9.2 | 0.25 | 0.055 | 4.9 | 3.1 | 15.5 5 | 2.03 | 371. 2 |

Table 3 presents the experimental parameters for a multiple-injection strategy implemented in a high-pressure diesel engine test. The injection sequence consists of three pilot injections and one main injection, each carefully defined by its start of injection (SOI), fuel fraction, injected mass, separation between pulses, injection duration, droplet size (d_{32}), ignition delay, and burst timing in crank angle degrees. The

first pilot injection begins at the earliest at 15° CA BTDC with 25% of the total fuel mass, followed by the second and third pilot injections with slightly higher and lower fuel fractions and shorter ignition delays. The main injection, timed at 9.2° CA BTDC, delivers the remaining 25% of the fuel to complete the cycle. This staged multi-pulse injection approach aims to control the fuel-air mixing and combustion phases more precisely, which helps to optimize heat release, reduce emissions, and improve combustion stability in modern diesel engines.

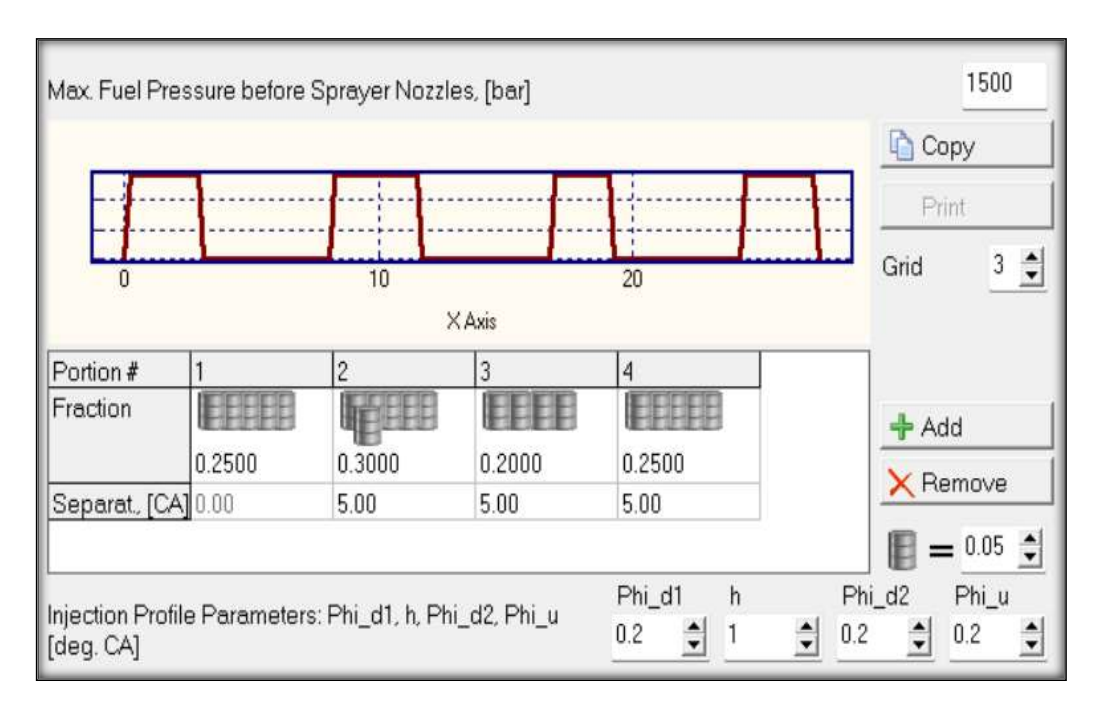


Figure 5: Split Injection Parameters strategy 1

The displayed fuel injection system configuration represents a custom multi-pulse injection strategy for a diesel engine using Diesel No. 2 fuel with a cycle fuel mass of 0.222 g and a maximum injection pressure of 1500 bar shown in Figure 5. The injection event is divided into four portions, with fractions of 25%, 30%, 20%, and 25% of the total fuel mass, respectively, each separated by 5 degrees of crank angle. This parametric split injection profile helps optimize the combustion process by precisely controlling fuel delivery timing and duration, which can reduce emissions such as NOx and particulate matter while improving combustion efficiency and thermal performance. The diagram shows how these injection pulses are distributed over the cycle, illustrating a modern strategy for achieving cleaner and more efficient diesel engine operation.

Table 4: Split Injection Parameters strategy-2 data

| Portion | SOI [CA BTDC] | Fraction | Mass [g] | Separation [CA] | Duration [CA] | d32 [μm] | Ign. Delay [CA] | Burst [CA] |
|---------|---------------------|----------|-------------|--------------------|------------------|-------------|-----------------------|---------------|
| Pilot 1 | 15 | 0.3 | 0.0666 | | 3.7 | 16.03 | 4.48 | 349.5 |
| Pilot 2 | 6.4 | 0.2 | 0.0444 | 4.9 | 2.6 | 15.58 | 2.96 | 356.6 |
| Main | -1.1 | 0.25 | 0.0555 | 4.9 | 3.2 | 15.3 | 2.12 | 363.2 |
| Post 1 | -9.2 | 0.25 | 0.0555 | 4.9 | 3.1 | 15.55 | 2.03 | 371.2 |

The multiple injection parameters summarized in Table 4 illustrate a carefully calibrated strategy involving four distinct fuel portions—two pilot injections, a main injection, and a post injection—to optimize combustion phasing and emissions control. The pilot injections, starting at 15.0° and 6.4° CA BTDC, account for 50% of the total fuel mass, initiating combustion smoothly and reducing ignition delay. The main injection at -1.1° CA BTDC supplies 25% of the fuel mass to sustain peak combustion pressure, while the post injection at -9.2° CA BTDC contributes the remaining 25%, aiding in soot oxidation and emission reduction. The droplet Sauter Mean Diameters (d32) indicate efficient atomization for each portion, supporting complete combustion. The fuel allocation analysis confirms that over 94% of the fuel impinges accurately within the piston bowl, with minimal losses to surrounding surfaces, while high evaporation constants for the dilution and spray core zones demonstrate rapid fuel vaporization for cleaner combustion.

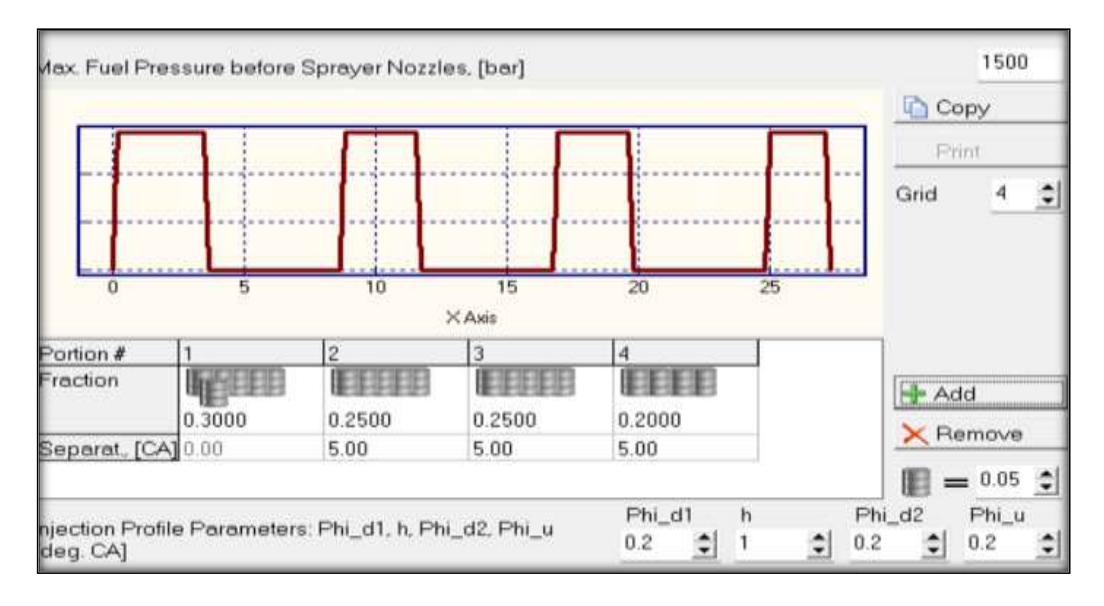


Figure 6: Split Injection Parameters and Strategy-2

The figure 6 illustrates a custom fuel injection system configuration in Diesel-RK, designed with a four-stage multiple injection strategy. The injection profile is defined parametrically, distributing the total fuel cycle mass into four portions: 30% for the first

pilot injection, 25% for the second, another 25% for the third, and 20% for the final main injection. The separation between each portion is maintained at 5 crank angle degrees, allowing for staggered delivery and enhanced control of combustion phasing. The injection pressure before the sprayer nozzles is set at 1500 bar to ensure fine atomization and efficient mixing within the combustion chamber. This carefully calibrated split injection approach aims to optimize ignition delay, reduce peak combustion temperatures, and achieve a more uniform heat release rate, ultimately targeting lower NOx emissions and improved fuel efficiency while maintaining combustion stability.

Table 5: Split Injection Parameters strategy-3 data

| Injectio n | SOI [CA BTDC | Fractio n | Mass [g] | Separ . [CA] | Duratio n [CA] | d32 [μm] | Ign. Dela y [CA] | Burs t [CA] |
|---------------|--------------------|--------------|-------------|-----------------|-------------------|-------------|---------------------------|-------------------|
| Pilot 1 | 15 | 0.25 | 0.055 | | 3.1 | 16.0 8 | 4.48 | 349.5 |
| Pilot 2 | 7 | 0.25 | 0.055 5 | 4.9 | 3.2 | 15.4 8 | 3.07 | 356.1 |
| Main | -1.1 | 0.25 | 0.055 5 | 4.9 | 3.2 | 15.2 9 | 2.11 | 363.2 |
| Post 1 | -9.2 | 0.25 | 0.055 5 | 4.9 | 3.1 | 15.5 5 | 2.02 | 371.2 |

The multiple injection parameters detailed above represent a carefully optimized injection strategy combining two pilot injections, a main injection, and a post-injection to enhance combustion efficiency and emissions control shown in Table 5. The sequential split of injection events—starting with a first pilot at 15° CA BTDC, followed by a second pilot at 7°, a main injection slightly after TDC at -1.1°, and a post injection at -9.2°—ensures a gradual and controlled release of fuel mass, each portion contributing equally with 0.250 fraction and 0.0555 g mass. The consistent droplet sizes (d32) around 15–16 µm and staggered ignition delays help achieve smoother combustion with reduced knocking tendencies. The fuel distribution confirms that the majority impinges inside the piston bowl (97.16%), ensuring proper mixing and minimal wall wetting, while the calculated evaporation constants reflect efficient atomization dynamics across combustion zones. This multi-stage injection profile is vital for modern diesel engines targeting lower NOx and PM emissions while maintaining high thermal efficiency.

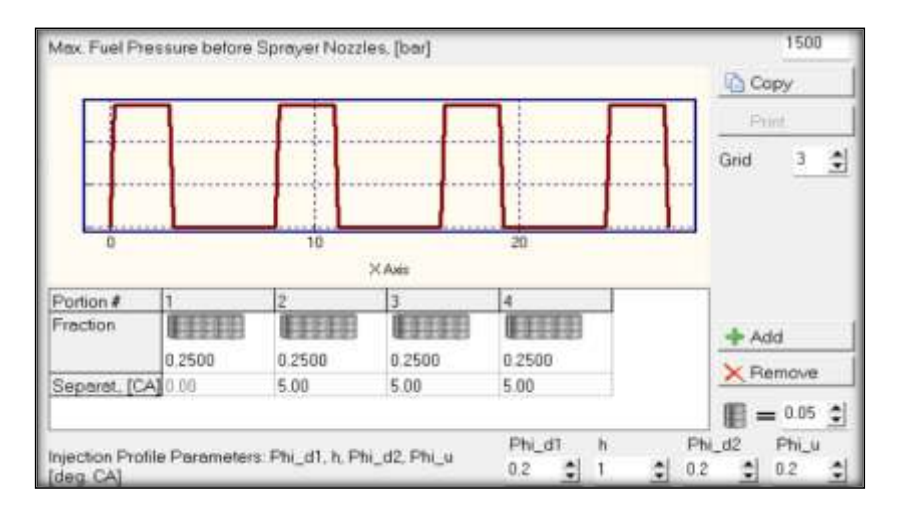


Figure 7: Split Injection Parameters and Strategy-3

The injection profile depicted in Strategy-3 represents a balanced multi-pulse injection strategy, where the total fuel mass is equally distributed across four portions, each contributing 25% of the cycle fuel mass shown in Figure 7. The injections are separated by a consistent crank angle interval of 5° CA, providing precise control over fuel delivery and combustion phasing. This uniform split promotes stable combustion and improved mixing, which helps achieve better thermal efficiency and reduced emission levels. The parametrically defined profile, with identical injection duration parameters (Phi_d1, h, Phi_d2, Phi_u), ensures that each injection pulse has a similar shape and duration, facilitating repeatable atomization and evaporation characteristics under high injection pressures. Such a strategy is especially useful in advanced diesel combustion systems targeting low soot and NOx emissions while maintaining robust engine performance.

3.3 COMPARISON OF PERFORMANCE PARAMETERS

| Table 6: Si | nlit In | iection | Parameters | strategy | comparison | data |
|-------------|---------|---------|---------------|------------|------------|------|
| Tuoic O. D | | CCLIOII | 1 alaminotors | bu acc _ , | companion | aata |

| Parameter | Fuel Injection Strategy 1 | Fuel Injection Strategy 2 | Fuel Injection Strategy 3 | Unit | Description |
|-----------|------------------------------------|------------------------------------|------------------------------------|---------|----------------------------------|
| RPM | 1500 | 1500 | 1500 | rev/min | Engine Speed |
| Peng | 41.75 | 41.712 | 41.789 | kW | Piston Engine Power |
| BMEP | 10.5 | 10.491 | 10.51 | bar | Brake Mean Effective Pressure |
| Torque | 265.81 | 265.56 | 266.06 | N·m | Brake Torque |

| mf | 0.222 | 0.222 | 0.222 | g | Mass of Fuel Supplied per Cycle |
|--------|---------|---------|---------|--------|--|
| SFC | 0.23928 | 0.2395 | 0.23906 | kg/kWh | Specific Fuel Consumption |
| SFCISO | 0.22605 | 0.22626 | 0.22585 | kg/kWh | Specific Fuel Consumption (ISO) |
| ηf | 0.354 | 0.35368 | 0.35434 | | Efficiency of Piston Engine |
| IMEP | 13.35 | 13.335 | 13.355 | bar | Indicated Mean Effective Pressure |
| ηi | 0.45007 | 0.44958 | 0.45024 | _ | Indicated Efficiency |
| Sp | 9 | 9 | 9 | m/s | Mean Piston Speed |
| FMEP | 2.1193 | 2.1194 | 2.1183 | bar | Friction Mean Effective Pressure |
| ηm | 0.83206 | 0.83192 | 0.83226 | | Mechanical Efficiency of Piston Engine |

Comparison Summary

Table 6 shows that the engine speed (RPM) and the mass of fuel supplied per cycle (mf) remain identical for all three strategies, indicating that the base operating conditions were kept constant to isolate the effect of different injection strategies. When comparing engine power (Peng) and torque, Strategy 3 shows the highest values (41.789 kW, 266.06 Nm), indicating a slight improvement in brake output compared to Strategies 1 and 2. Strategy 2 shows the lowest torque and power, implying a marginally less effective energy conversion for the same fuel mass.

The Brake Mean Effective Pressure (BMEP) and Indicated Mean Effective Pressure (IMEP) follow the same trend — Strategy 3 slightly outperforms the others, suggesting better in-cylinder pressure development. In terms of fuel efficiency, the Specific Fuel Consumption (SFC) and SFC (ISO) are lowest for Strategy 3 (0.23906 kg/kWh and 0.22585 kg/kWh, respectively), implying that Strategy 3 converts fuel energy into brake power more effectively. The overall piston engine efficiency (ηf) and indicated efficiency (ηi) are also slightly highest for Strategy 3 (0.35434 and 0.45024), reinforcing this observation. Mean Piston Speed (Sp) remains constant (9 m/s) for all, which makes sense because the engine speed is fixed. Finally, the Friction Mean Effective Pressure (FMEP) is marginally lower for Strategy 3 (2.1183 bar) than for Strategies 1 and 2, which slightly improves the mechanical efficiency (ηm) to 0.83226 — again, the best among the three. Fuel Injection Strategy 3 achieves the best balance among power output, torque, fuel consumption, and overall efficiency under the same operating conditions. Although the differences are subtle, they highlight the impact of optimizing injection timing, splitting, or mass fraction on combustion quality and mechanical performance.

3.4 COMPARISON OF COMBUSTION PARAMETERS

Table 7: Combustion Parameters Data

Diesel fuel

| Combustio | Fuel | Fuel | Fuel | Unit | Description |
|-----------------|-----------|-----------|-----------|-------------------|-------------------------------------|
| n | injection | injection | injection | | • |
| Parameters | Startegy | Startegy | Startegy | | |
| A /IE | 1.5026 | 1.5020 | 1.5001 | | A: E 1E : 1 |
| A/F_eq | 1.5036 | 1.5038 | 1.5081 | _ | Air-Fuel Equivalence |
| F/A_eq | 0.66506 | 0.66497 | 0.66311 | | Ratio (Lambda) Fuel-Air Equivalence |
| r/A_eq | | | | | Ratio |
| p_max | 129.64 | 130.43 | 129.94 | bar | Maximum Cylinder Pressure |
| T_max | 1929.6 | 1924.5 | 1925.5 | K | Maximum Cylinder |
| | | | | | Temperature |
| CA_p.max | 7 | 7 | 7 | deg. | Angle of Max. Cylinder |
| | | | | A.TD | Pressure |
| | | | | С | |
| CA_t.max | 18 | 18 | 18 | deg. | Angle of Max. Cylinder |
| | | | | A.TD | Temperature |
| 1 / 1751 4 | 5 1 (22 | 5 1556 | 5.0379 | C bar/de | M D (CD |
| dp/dTheta | 5.1632 | 5.1556 | 5.03/9 | | Max. Rate of Pressure |
| Ring Intn | 1.3236 | 1.31 | 1.2559 | g MW/m | Rise Ringing / Knock |
| King_Inth | 1.3230 | 1.31 | 1.2339 | 1V1 VV / III 2 | Intensity |
| F max | 23208 | 23349 | 23261 | kg | Max. Gas Force on |
| T_max | 23200 | 23347 | 23201 | Kg | Piston |
| p_inj.max | 1544.5 | 1545.4 | 1544.5 | bar | Max. Sac Injection |
| 1 _ 3 | | | | | Pressure |
| p_inj.avr | 1341.8 | 1340.3 | 1341.2 | bar | Mean Sac Pressure |
| d ₃₂ | 15.611 | 15.637 | 15.6 | μm | Sauter Mean Diameter |
| | | | | | of Drops |
| SOI | 15 | 15 | 15 | deg. | Start of |
| | | | | B.TDC | Injection/Ignition |
| | | | | | Timing |
| Phi_inj | 27.3 | 27.3 | 27.3 | CA | Duration of Injection |
| | 0.0 | 0.0 | 0.2 | deg. | D 1 00 10 |
| Phi_d1 | 0.2 | 0.2 | 0.2 | CA | Duration of First Phase |
| DL: : | 1 1 (1 | 4.4027 | 4.4015 | deg. | Fuel Flow Rise |
| Phi_ign | 4.464 | 4.4827 | 4.4815 | deg. | Ignition Delay Period |

| SOC | 10.536 | 10.517 | 10.518 | deg. B.TDC | Start of Combustion |
|--------------------|---------|---------|---------|---------------|---|
| x _e .id | 0.12437 | 0.13239 | 0.12432 | | Fuel Mass Fraction Evaporated during Ignition Delay |
| Phi_z | 142 | 142 | 141 | deg. | Combustion Duration |
| Rs_tdc | 0.1 | 0.1 | 0.1 | _ | Swirl Ratio at TDC |
| Rs_ivc | 0.07737 | 0.07699 | 0.07764 | | Swirl Ratio at IVC |
| W_swirl | 0.96893 | 0.96893 | 0.96893 | m/s | Max. Air Swirl Velocity at Cylinder R=62 mm |

The comparative analysis of diesel combustion parameters for three fuel injection strategies is shown in Table 7, and compares the minimal yet insightful variations in key metrics. The air-fuel equivalence ratio (A/F eq) ranged from 1.5036 to 1.5081, indicating consistent stoichiometry across strategies. Maximum cylinder pressure slightly increased from 129.64 bar for Strategy 1 to 130.43 bar for Strategy 2, before stabilizing at 129.94 bar for Strategy 3. The peak cylinder temperature remained steady, with values between 1924.5 K and 1929.6 K. The maximum rate of pressure rise decreased marginally from 5.1632 bar/deg to 5.0379 bar/deg, showing smoother combustion for Strategy 3. Ringing intensity reduced from 1.3236 MW/m² to 1.2559 MW/m², highlighting improved knock resistance. The maximum gas force on the piston peaked at 23,349 kg in Strategy 2. Injection pressures stayed consistent, around 1544–1545 bar for maximum sac pressure and 1340–1341 bar for mean sac pressure. The Sauter mean diameter (d₃₂) of fuel droplets varied slightly between 15.6–15.637 µm. Ignition delay (Phi ign) hovered around 4.46-4.48°, and the combustion duration (Phi z) shortened marginally from 142°CA to 141°CA. Swirl ratios and maximum air swirl velocity remained constant at 0.1 and 0.96893 m/s, respectively, indicating stable air motion characteristics throughout all strategies.

Based on the detailed comparison of combustion parameters for diesel fuel under the three fuel injection strategies, it is evident that Fuel Injection Strategy 2 demonstrates slightly superior combustion characteristics. It achieves the highest maximum cylinder pressure at 130.43 bar, indicating efficient fuel energy conversion, and generates the greatest maximum gas force on the piston at 23,349 kg, which contributes to effective power output. Despite a minimal increase in ignition delay (4.4827°) compared to Strategy 1, Strategy 2 maintains a favourable air-fuel ratio (1.5038) and achieves a slightly lower ringing intensity (1.31 MW/m²), suggesting reduced knock tendency. Overall, the combination of higher peak pressure, better gas force, and controlled knock tendency makes Fuel Injection Strategy 2 the preferable choice for optimal combustion performance under the tested conditions.

4. 0 UNCERTAINTY ANALYSIS

| | Table 8: | Uncertainty | Analysis |
|--|----------|-------------|-----------------|
|--|----------|-------------|-----------------|

| Parame ter | Value (EGR = 0.0000) ± Uncertai nty | Value (EGR = 0.0500) ± Uncertai nty | Value (EGR = 0.1000) ± Uncertai nty | Value (EGR = 0.1500) ± Uncertai nty | Value (EGR = 0.2000) ± Uncertai nty | Value (EGR = 0.2500) ± Uncertai nty |
|---------------|---|---|---|---|---|---|
| A/F_eq | 2.4512 ± 0.01 | 2.3919 ± 0.01 | 2.3261 ± 0.01 | 2.2532 ± 0.01 | 2.1718 ± 0.01 | 2.0932 ± 0.01 |
| P_eng | 28.724 ± 0.05 | 28.515 ± 0.05 | 28.335 ± 0.05 | 28.123 ± 0.05 | 27.910 ± 0.05 | 27.698 ± 0.05 |
| SFC | 0.3478 ± 0.001 | 0.3503 ± 0.001 | 0.3526 ± 0.001 | 0.3552 ± 0.001 | 0.3579 ± 0.001 | 0.3606 ± 0.001 |
| Torque | 182.87 ± 0.1 | 181.55 ± 0.1 | 180.40 ± 0.1 | 179.05 ± 0.1 | 177.70 ± 0.1 | 176.20 ± 0.1 |

To perform an uncertainty analysis for the provided data shown in Table 8, and need to compute the uncertainties for each parameter. Here's a step-by-step explanation of how the table for uncertainty analysis can be constructed:

Determine Uncertainty Sources: Consider potential sources of uncertainty in the experimental or simulation data, such as measurement error, equipment tolerance, or modeling approximations. Calculate Uncertainty: For each parameter at each EGR level, calculate the mean value. Determine the standard deviation if multiple measurements are available. If not, estimate based on known tolerances or specifications. Express Uncertainty: Represent the uncertainty using absolute or relative terms (e.g., $\pm 0.5\%$ or ± 0.02). Construct Table 8: Include the parameter values, their respective uncertainties, and the methodology used to compute the uncertainties

Conclusion

- Engine Power: Among the three strategies, Fuel Injection Strategy 3 delivered the highest piston engine power at 41.789 kW, slightly higher than Strategy 1 (41.75 kW) and Strategy 2 (41.712 kW). This shows an improvement of about 0.09% compared to Strategy 1.
- Brake Torque: Strategy 3 produced the highest brake torque of 266.06 Nm, compared to 265.81 Nm (Strategy 1) and 265.56 Nm (Strategy 2). This represents a torque improvement of approximately 0.19% over Strategy 2.
- Fuel Efficiency (SFC): The lowest Specific Fuel Consumption was observed in Strategy 3 at 0.23906 kg/kWh, which is marginally lower than Strategy 1 (0.23928 kg/kWh) and Strategy 2 (0.2395 kg/kWh), indicating improved fuel utilization efficiency.

- Combustion Efficiency: The Indicated Mean Effective Pressure (IMEP) was highest for Strategy 3 at 13.355 bar, slightly above Strategy 1 (13.35 bar) and Strategy 2 (13.335 bar). A higher IMEP reflects more effective combustion and better pressure development in the cylinder.
- Mechanical Efficiency: The mechanical efficiency (ηm) of the piston engine reached 0.83226 for Strategy 3, outperforming Strategy 1 (0.83206) and Strategy 2 (0.83192). This indicates reduced friction losses, confirmed by Strategy 3 having the lowest FMEP (2.1183 bar) compared to 2.1193 bar and 2.1194 bar.
- Overall, Balance: Combining these results, Strategy 3 shows a slight but consistent advantage in power, torque, fuel consumption, and efficiency parameters. This demonstrates that a refined injection strategy can yield measurable gains even small numerical improvements in thermal and mechanical efficiency can significantly impact long-term fuel savings and performance stability.

Acknowledgment

The authors wish to express their sincere gratitude to Dr. A. Karthikeyan, Dr. M. Karthikeyan, and Dr. G. Sureshkannan, Assistant Professors and Associate Professors in the Department of Mechanical Engineering, Coimbatore Institute of Technology, Coimbatore-14, for their invaluable guidance, unwavering support, and constant encouragement throughout this research. The authors also extend their heartfelt thanks to the Principal of Coimbatore Institute of Technology and Management for providing the essential facilities, resources, and support that contributed to the successful completion of this study.

NOMENCLATURE

- CR: Compression Ratio
- **BMEP**: Brake Mean Effective Pressure (bar)
- P eng: Piston Engine Power (kW)
- **Torque**: Brake Torque (N·m)
- SFC: Specific Fuel Consumption (kg/kWh)
- **IMEP**: Indicated Mean Effective Pressure (bar)
- A/F eq: Air-Fuel Equivalence Ratio (Lambda) in the Cylinder
- To T: Average Total Turbine Inlet Temperature (K)
- Tw pist: Average Piston Crown Temperature (K)

- P inj.max: Maximum Sac Injection Pressure (before nozzles) (bar)
- **d_32**: Sauter Mean Diameter of Drops (microns)
- **Phi_ign**: Ignition Delay Period (degrees)
- P max: Maximum Cylinder Pressure (bar)
- **dp/dTheta**: Maximum Rate of Pressure Rise (bar/degree)
- **Phi_z**: Combustion Duration (degrees)
- m air: Total Mass Airflow (+EGR) of Piston Engine (kg/s)
- Eta v: Volumetric Efficiency
- x r: Residual Gas Mass Fraction
- **PMEP**: Pumping Mean Effective Pressure (bar)
- Eta TC: Turbocharger Efficiency
- **BF int**: Burnt Gas Fraction Backflowed into the Intake (%)
- **NOx.ppm**: Fraction of Wet NOx in Exhaust Gas (ppm)
- PM: Specific Particulate Matter Emission (g/kWh)
- **Bosch**: Bosch Smoke Number
- SE: Summary of Emission of PM and NOx
- A egr: Effective Area of EGR Discharge Holes (mm²)
- **dp** ev: Differential Pressure between Exhaust Manifold and Venturi Throat (bar)
- P C.hp: Power of High-Pressure Compressor (HPC) (kW)
- To_C.hp: Total Temperature After Intercooler (K)
- **PR T.hp**: Expansion Pressure Ratio of High-Pressure Turbine (HPT)
- **Eta T.hp**: Internal Turbine Efficiency of High-Pressure Turbine
- **P** T.hp: Effective Power of High-Pressure Turbine (kW)
- p o.I.hp: Inlet Total Pressure of High-Pressure Turbine (bar)

- To I.hp: Inlet Total Temperature of High-Pressure Turbine (K)
- RPM_C.hp: HP Stage Turbocharger Rotor Spee

References

- 1. Heywood, J. B. Internal Combustion Engine Fundamentals. McGraw-Hill Education, 1988.
- 2. Rakopoulos, C. D., & Dimaratos, A. M. (2012). Experimental study of combustion and emissions of a HSDI diesel engine using pilot fuel injection. Energy, 43(1), 392–403.
- 3. Payri, F., Bermúdez, V., Payri, R., & Salvador, F. J. (2004). The influence of cavitation on the internal flow and the spray characteristics in diesel injection nozzles. Fuel, 83(4–5), 419–431.
- 4. Desantes, J. M., Pastor, J. V., García-Oliver, J. M., & Pastor, J. M. (2011). Influence of the mass fraction burned of multiple injections on DI diesel engine combustion and emissions. Energy Conversion and Management, 52(1), 278–287.
- 5. Zhou, D., Xu, H., & Ma, X. (2013). Effect of injection strategies on performance, combustion and emissions of a diesel engine fuelled with biodiesel. Renewable Energy, 57, 469–475.
- 6. Kim, D., & Bae, C. (2012). Combustion and emission characteristics of biodiesel in a direct injection diesel engine with pilot injection. Fuel, 97, 504–510.
- 7. Li, Z., Zhang, L., & Li, C. (2014). The effects of pilot injection timing and quantity on combustion and emissions in a diesel engine. Energy Conversion and Management, 79, 114–121.
- 8. Lee, C. S., Park, S. W., & Kwon, S. (2005). An experimental study on the atomization and combustion characteristics of biodiesel-blended fuels. Energy & Fuels, 19(5), 2201–2208.
- 9. Agarwal, A. K., & Dhar, A. (2013). Experimental investigations of performance, emission and combustion characteristics of Karanja oil blends in a direct injection compression ignition engine. Renewable Energy, 52, 283–291.
- 10. Ganapathy, T., Murugesan, K., & Gakkhar, R. P. (2011). Performance optimization of Jatropha biodiesel engine model using particle swarm optimization. Energy, 36(2), 1228–1236.
- 11. Gao, Y., & Zhang, L. (2016). Effect of split injection on combustion and emissions in diesel engines: A review. Renewable and Sustainable Energy Reviews, 60, 433–441.
- 12. Papagiannakis, R. G., & Hountalas, D. T. (2003). Combustion and exhaust emission characteristics of a dual fuel compression ignition engine operated with pilot diesel fuel and natural gas. Energy Conversion and Management, 44(18), 3025–3042.
- 13. Rakopoulos, C. D., & Giakoumis, E. G. (2007). Diesel Engine Transient Operation: Principles of Operation and Simulation Analysis. Springer.
- 14. Witze, P. O., & Harrington, D. L. (1982). The effect of injection timing and pressure on diesel combustion and emissions. SAE Technical Paper 820345.
- 15. Kuti, O. A., Nishida, K., & Ogawa, H. (2011). Experimental investigation of the spray characteristics of biodiesel fuel using a constant volume chamber. Experimental Thermal and Fluid Science, 35(3), 660–667.
- 16. Park, S. H., Lee, C. S., & Song, S. (2010). Effects of multiple-injection strategies on overall spray behavior, combustion, and emissions reduction characteristics of biodiesel fuel. Energy & Fuels, 24(2), 710–718.
- 17. Chen, Z., Liu, J., & Shuai, S. (2012). Effects of split injection on combustion and emissions under different pilot-main injection ratios. Fuel, 95, 324–331.

- 18. Zheng, M., Reader, G. T., & Hawley, J. G. (2004). Diesel engine exhaust gas recirculation—A review on advanced and novel concepts. Energy Conversion and Management, 45(6), 883–900.
- 19. Musculus, M. P. B., Miles, P. C., & Pickett, L. M. (2013). Conceptual models for partially premixed low-temperature diesel combustion. Progress in Energy and Combustion Science, 39(2–3), 246–283.
- 20. Hardenberg, H. O., & Hase, F. W. (1979). An empirical formula for computing the pressure rise delay of a fuel oil from its cetane number and from the relevant parameters of directinjection diesel engines. SAE Technical Paper 790493.
- 21. Lapuerta, M., Armas, O., & Rodríguez-Fernández, J. (2008). Effect of biodiesel fuels on diesel engine emissions. Progress in Energy and Combustion Science, 34(2), 198–223.
- 22. Tree, D. R., & Svensson, K. I. (2007). Soot processes in compression ignition engines. Progress in Energy and Combustion Science, 33(3), 272–309.
- 23. Sahoo, B. B., Sahoo, N., & Saha, U. K. (2009). Effect of engine parameters and type of gaseous fuel on the performance of dual-fuel gas diesel engines—A critical review. Renewable and Sustainable Energy Reviews, 13(6–7), 1151–1184.
- 24. Roy, M. M., Wang, W., & Bujold, J. (2014). A study on the performance and emissions of a diesel engine fuelled with biodiesel-diesel blends and combustion additives. Fuel, 115, 702–708.
- 25. Kegl, B. (2008). Effects of biodiesel on emissions of a bus diesel engine. Bioresource Technology, 99(4), 863–873.
- 26. Kannan, G. R., Anand, R., & Mahalakshmi, N. V. (2009). Experimental studies on the combustion and emission characteristics of a diesel engine fuelled with pongamia pinnata methyl ester and its blends. Energy, 34(10), 1613–1621.
- 27. Zajac, G., & Wislocki, K. (2005). The effect of injection timing and swirl on emissions and combustion in a DI diesel engine. Combustion Engines, 122, 3–12.
- 28. Foucher, F., Pierre, C., Mounaïm-Rousselle, C., & Lahaye, J. (2009). Effects of multiple injection strategies on combustion and emissions for an automotive diesel engine. Fuel, 88(4), 695–703.
- 29. Benajes, J., García, A., Monsalve-Serrano, J., & Durrett, R. P. (2016). An investigation on RCCI combustion at low load, enabled by a closed-loop combustion control system. Applied Energy, 162, 179–191.
- 30. Reitz, R. D., & Duraisamy, G. (2015). Review of high efficiency and clean reactivity-controlled compression ignition (RCCI) combustion in internal combustion engines. Progress in Energy and Combustion Science, 46, 12–71.